

The internal bremsstrahlung spectrum in the unique first-forbidden K -capture decay of ^{204}Tl

A. Zide and H. Lancman

Brooklyn College of the City University of New York, Brooklyn, New York 11210

(Received 1 November 1978)

The spectrum of the internal bremsstrahlung accompanying the K -capture decay of ^{204}Tl was measured. The intensity of the spectrum in the range from 103 keV to the end point was found to be $(2.17 \pm 0.26) \times 10^{-5}$ photons per K capture, 4.3 times lower than the intensity predicted by the theory of Zon. The Coulomb-free version of the theory is in better agreement with the data.

[RADIOACTIVITY ^{204}Tl ; measured IB x-ray coin; deduced I_{IB} , Q .]

I. INTRODUCTION

Internal bremsstrahlung (IB) accompanying capture of orbital electrons has been extensively investigated for allowed transitions. Morrison and Schiff¹ developed the early theory of the IB spectrum using the highly simplified assumptions that the effect of the nuclear Coulomb field on the intermediate electron states may be neglected, and that capture takes place only from the K shell. Considerable improvement of the theory was made by Martin and Glauber.^{2,3} They took into account Coulomb and relativistic effects as well as screening and included capture from L and M shells. A recent review of the experimental results was given by Bambynek *et al.*⁴

The theory of forbidden transitions was developed by Zon and Rapoport⁵ and later by Zon⁶ who presented formulas for the IB spectra accompanying capture from an arbitrary shell and valid to any degree of forbiddenness. For verification of this theory, unique first-forbidden transitions are of great interest since in this case the intensity of IB per nonradiative capture does not depend on matrix elements involving nuclear wave functions. Two such transitions have been studied. Myslek *et al.*⁷ have measured the IB spectrum in the decay of ^{41}Ca and found that its shape does not agree with the theory. Lancman and Bond⁸ have determined the IB spectrum accompanying K -electron capture in ^{204}Tl . In the latter work the IB spectrum was measured in coincidence with Hg x rays; however, the use of NaI(Tl) detectors for both the x rays and the IB made it impossible to estimate accurately the contributions of other higher order effects to the measured IB spectrum. The results of this measurement were not, therefore, compared with the predictions of the Zon and Rapoport theory.

The purpose of the present work was to carry out the measurement of the IB in a way that would allow an accurate separation of these contributions. This was done by employing a high-resolution Ge(Li) spectrometer in the x-ray branch of the system. A careful examination of the x-ray spectrum, which this made possible, revealed contributions not only due to double internal and external bremsstrahlung which were discussed previously⁸ but also due to internal bremsstrahlung accompanying K -shell autoionization in the β^- decay of ^{204}Tl , a new effect which has not been reported before.⁹

Investigations of IB for allowed K -capture transitions have shown that its intensity depends on the nuclear charge Z as a result of Coulomb and relativistic effects. The Martin and Glauber theory has successfully accounted for these effects by a correction factor R_{1s} which multiplies the Morrison and Schiff expression. This factor has only a small influence on the shape of the spectrum. It was of interest to consider the effect of Z in the Zon and Rapoport theory, and compare the experimental spectrum to a Coulomb-free version of this theory. This is obtained by setting $Z=0$ in the expression given by Zon and leads to a spectral distribution of the IB identical to that obtained by application of the Cutkosky rule.¹⁰

In contrast to the situation in allowed transitions the Coulomb-free version of the theory gives a lower intensity for the IB spectrum of ^{204}Tl than the full theory. As will be shown the Coulomb-free theory is in better agreement with our experimental results.

The spectra predicted by the theory and its Coulomb-free version are shown in Fig. 1(a) and 1(b), respectively, for several values of K_m , the end-point energy. The comparison of the experi-

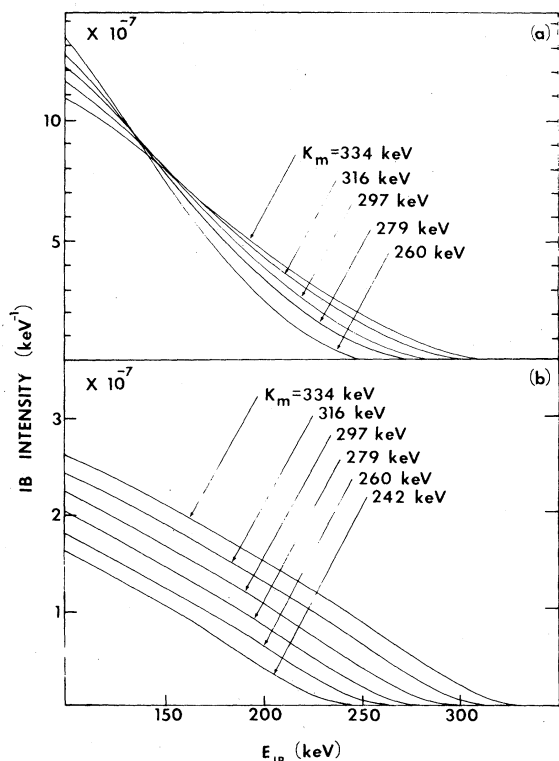


FIG. 1. IB spectra accompanying K capture in ^{204}Tl for various end-point energies: (a) obtained with $R_{1s}^{(1)}$ and $R_{1s}^{(2)}$ given by Zon (Ref. 17); (b) obtained with $R_{1s}^{(1)} = R_{1s}^{(2)} = 1$, ($Z = 0$).

mental data and the Coulomb-free theory gives a lower K_m for the IB spectrum of ^{204}Tl than a similar comparison made with the full theory. For this reason the Coulomb-free spectra were computed starting from a lower end-point energy.

II. EXPERIMENTAL APPARATUS AND PROCEDURES

The IB spectrum was measured with a 7.6×7.6 cm NaI(Tl) detector. The x rays were measured with an Ortec high resolution Ge(Li) detector with a 0.125 mm thick Be window. The sensitive region of the detector was 16 mm in diameter and 5 mm thick. To obtain a satisfactory coincidence counting rate it was necessary to place the detectors face to face. This arrangement resulted in serious backscattering from one detector to the other. To minimize this backscattering a set of conical collimators was used. The source, covered on both sides by beryllium discs, was centered between the collimators as shown in Fig. 2. The whole setup was placed in a lead housing of 5 cm wall thickness to reduce the background.

A ^{204}Tl source with a strength of 18 300 Hg K x rays per second was used to collect the data for

a total time of 329.5 h. The source, less than 2 mm in diameter, was evaporated on plastic tape and sealed in place. A special effort was made to achieve a uniform distribution of source material. The sources used for detector calibration were prepared in the same way and were approximately of the same intensity.

The ^{204}Tl source was examined for impurities in the energy range from 65 to 600 keV with the aid of a high resolution Ge(Li) spectrometer. The photon spectrum from ^{204}Tl consisted of Hg x rays superimposed on a continuous bremsstrahlung spectrum. No indications of impurities were detected. The upper limit of the intensity of contaminant γ rays was found to be 2×10^{-7} per decay of ^{204}Tl .

The electronics consisted of a fast-slow coincidence system. Slow pulses from the NaI(Tl) detector were gated on bremsstrahlung in the energy interval from 90 to 600 keV; the Ge(Li) detector pulses were gated on the region including the Hg $K\alpha$ and $K\beta$ x rays, which spanned the energy interval from 65 to 87 keV. A biased amplifier was included in the x-ray branch to distribute the narrow band of pulses along the 64 channels available for x-ray analysis.

The gate pulses determined a slow coincidence, which was used to strobe the output of the time-to-amplitude converter (TAC). The "start" and "stop" pulses used to drive the TAC were developed in constant fraction timing discriminators in either branch of the system. It proved advantageous to start the TAC with the Ge(Li) pulses and stop it with the fast pulses from the RCA 8575 tube coupled to the NaI(Tl) detector. The TAC coincidence spectrum accumulated during the run had a full width at half maximum (FWHM) of 13 ns.

A ^{207}Bi source was used to determine the efficiency of the coincidence electronics. The decay

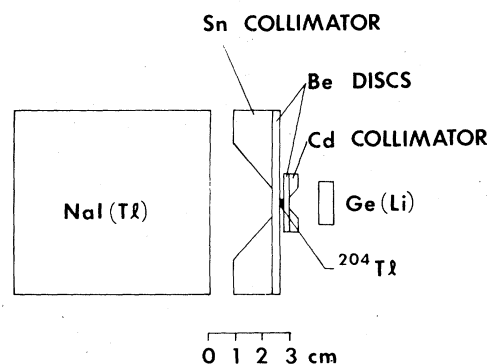


FIG. 2. Experimental arrangement of the ^{204}Tl source and the detectors.

of ^{207}Bi yields a high rate of coincidences between ^{207}Pb K x rays and 570 keV γ rays and therefore is ideally suited for the measurement since the energies of these photons lie within the ranges selected in the single channel analyzers for the IB measurements. A coincidence efficiency of practically 100% was found down to NaI(Tl) pulses of 90 keV.

The NaI(Tl) detector response functions and energy calibration were determined by measuring the pulse-height spectra resulting from a number of monoenergetic γ rays in the same experimental geometry as the one used for the IB measurements. The response for arbitrary energies was determined by interpolating over the characteristic components of these spectra; e.g., photopeak, Compton distribution, backscatter, and iodine x-ray escape peak. The photopeaks and escape peaks were fitted to Gaussian shapes. Because of the close geometry employed in the experiment, the Compton regions were divided into sections and the interpolation was carried out separately over each section. In addition, since tables of peak-to-total ratios are suitable under conditions of minimum scatter, these ratios were measured under the present experimental conditions. This procedure more accurately accounted for the shape and magnitude of the Compton distributions than fitting to geometrical shapes and thus assured that the effects associated with the close geometry were more accurately accounted for.

III. RESULTS AND DISCUSSION

The coincidence data were obtained simultaneously in trues and randoms in a two-parameter analysis mode. The data was arranged in 32×64 matrix arrays. The axes of the matrix represented the energies of the coincident photons, with the shorter dimension used for the NaI(Tl) spectra. Each of the 32 rows of the matrix represented a Ge(Li) spectrum corresponding to one channel of the NaI(Tl) spectrum. Figure 3 shows several representative spectra of the matrix obtained after subtraction of random coincidences. The latter accounted for about a half of the total coincidence data.

The prominent features of the spectra are the Hg $K\alpha$ and $K\beta$ x-ray peaks, which are superimposed on a continuous background mainly due to double internal bremsstrahlung¹¹ accompanying the decay of ^{204}Tl . The Ge(Li) detector allowed resolution of these x rays into their partial $K\alpha_1$, $K\alpha_2$, $K\beta_1$, and $K\beta_2$ components.

In order to demonstrate more clearly the presence of all the Hg K x-ray components in the co-

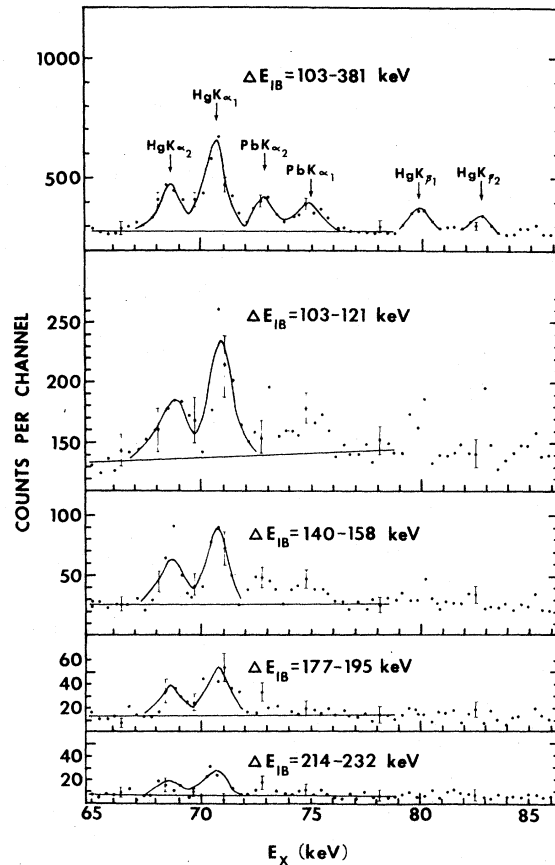


FIG. 3. Spectra of x rays obtained in coincidence with IB photons. The photon energy intervals ΔE_{IB} are indicated for each spectrum. The straight line under the K x-ray peaks is an interpolation of the smooth background due primarily to double internal bremsstrahlung.

incidence data spectra corresponding to bremsstrahlung in the energy range 103–381 keV were combined and the sum presented in the upper part of Fig. 3. The positions and the relative intensities of the peaks representing Hg x rays in this spectrum were found to be in good agreement with the singles spectrum. The relative intensities of the peaks were also compared to Salam's¹² theoretical calculations of the ratios of the x-ray transition probabilities. The agreement was satisfactory after corrections for the variation in detector efficiency and the germanium x-ray escape probability in the experimental data were taken into account.

The peaks at 72.9 and 74.9 keV which are very weak in the singles spectrum were identified as Pb $K\alpha$ x rays resulting primarily from autoionization accompanying IB in the β decay of ^{204}Tl , an effect which will be discussed in a separate paper.⁹

The IB intensities in the coincidence spectra

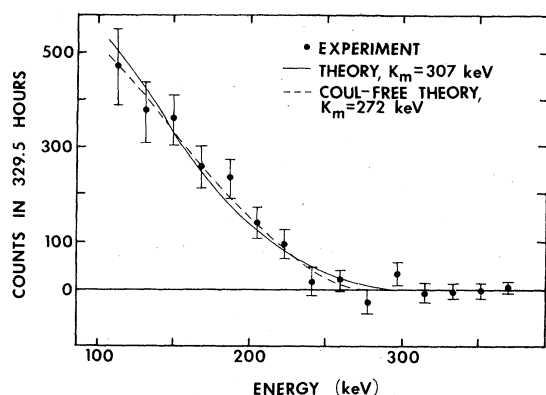


FIG. 4. Comparison of the experimental and theoretical 1s IB pulse height spectra of ^{204}Tl .

were determined by summing over the channels of the $K\alpha$ x-ray peaks, whose positions were determined from the singles spectra and subtracting the background, shown in Fig. 3 by the straight lines. The lines were obtained by a least squares fit. The Hg K x-ray intensities from this procedure were determined for the spectra corresponding to the IB in the energy range from 103 to 400 keV. The total K x-ray intensities which give the IB pulse-height distribution were obtained by multiplying the $K\alpha$ intensities by the $(K\alpha + K\beta)/K\alpha$ ratio. The resulting spectrum is shown in Fig. 4.

In order to compare the theoretical spectra to the experimental data, the theoretical spectra for a number of end-point energies were multiplied by the response matrix of the NaI(Tl) detector. The resulting pulse-height spectra were then normalized to the intensity of the experimental spectrum and compared to the latter in a χ^2 analysis.¹³ From the minimum value of χ^2 the end-point energy of the best fitting theoretical spectrum was determined for the full theory and for its Coulomb-free version. The best fitting theoretical pulse-

height spectra are shown in Fig. 4. For the full theory the minimum χ^2 obtained for the 15 experimental points was 13, corresponding to a spectrum end-point energy $K_m = 307 \pm 15$ keV. The normalization resulted in a theoretical to experimental intensity ratio of 4.3. The integrated intensity of the theoretical spectrum over the energy range 103–307 keV is 9.36×10^{-5} photons per K capture as compared to the experimental value of $(2.17 \pm 0.26) \times 10^{-5}$. The experimental error includes a 7% uncertainty in the intensity of the measured spectrum due primarily to counting statistics; a 5% uncertainty in the source intensity; a 6% uncertainty in the efficiency of the Ge(Li) detector; a 4% uncertainty in the response matrix which was primarily due to the uncertainties in the NaI(Tl) total detector efficiency and the experimentally determined peak-to-total ratios; and finally a 3% uncertainty in the system coincidence efficiency.

For the Coulomb-free theory the minimum χ^2 obtained was 9, corresponding to a value of $K_m = 272 \pm 15$ keV. The normalization condition yielded a ratio of 0.75 for the theoretical to experimental intensity. The intensity of the theoretical spectrum over the energy interval 103 to 272 keV was 1.62×10^{-5} photons per K capture per second.

The intensity measured by Lancman and Bond⁸ in the energy range 103 to 300 keV is $(3.2 \pm 0.5) \times 10^{-5}$ IB photons per K capture. The higher value than the one obtained in the present experiment is due to the fact that in the experiment of Lancman and Bond the two effects that contribute to the bremsstrahlung spectrum, K capture, and autoionization, could not be resolved.

The experimental results and theoretical predictions for ^{204}Tl are summarized in Table I. Results of earlier IB measurements,^{14,15} which served to determine the end-point energy appear to have been unreliable⁸ and therefore were not

TABLE I. Intensity and end-point energy of the K -capture IB spectrum in ^{204}Tl .

	Experiment			Theory	
	This work	Ref. 8	Ref. 17	Ref. 17 $Z=0$	Ref. 3
K_m (keV)	307 \pm 15 ^b	300 \pm 20 ^d			
Intensity ^a (10^{-5} phot./ K capt.)	272 \pm 15 ^c 2.17 \pm 0.26		3.2 \pm 0.5	9.36 ^e	1.62 ^f 1.0 ^g

^a Integrated over the energy range from 103 keV to the endpoint of the spectrum.

^b Based on a fit to the results of Zon's (Ref. 17) calculations.

^c Based on a fit to the Coulomb-free version of the theory.

^d Based on a fit to the Martin and Glauber theory.

^e Calculated for $K_m = 307$ keV.

^f Calculated for $K_m = 272$ keV.

^g Calculated for $K_m = 300$ keV.

included in Table I.

The comparison with Zon's theory yields a transition energy of 392 ± 15 keV in agreement with the value of 385 ± 20 keV obtained by Lancman and Bond.⁸ In the latter experiment the Martin and Glauber theoretical spectra for allowed transitions with the relativistic correction factor R_{1s} taken to be constant were used to obtain the end-point energy. The value obtained using the Coulomb-free spectra is 357 ± 15 keV. This is in satisfactory agreement with the value of 344 ± 8 keV given in the mass tables of Wapstra and Gove.¹⁶ It is clear that the transition energy depends strongly on the theoretical spectrum used in the comparison.

The shape of the measured spectrum is, within the accuracy of the data, in good agreement with both versions of the theory, the Coulomb-free approach yielding a slightly better fit. The two versions, however, disagree sharply on the magnitude of the effect. The intensity of the Zon theoretical spectrum is almost six times that of the Coulomb-free spectrum, the latter being closer to the experimental value. Part of the reason for this difference is due to the fact that the two theories yield different end-point energies. The intensities of the Coulomb-free spectra show a marked dependence on end-point energy as can be seen in Fig. 1(b). However, this dependence is not large enough to account for the discrepancy. In addition, as can be seen from Fig. 1(a), the intensities of the spectra obtained from using the full theory show very little change with changes in K_m . In order to have confidence in the results of these comparisons, the values of $R_{1s}^{(1)}$ and $R_{1s}^{(2)}$

calculated by Zon,¹⁷ which were used to determine the IB intensities have been checked independently by computer calculations.¹⁸ Excellent agreement was obtained.

The lack of agreement between the intensities of the experimental and the theoretical spectra might be due to detour transitions¹⁹⁻²¹ which were not considered in Zon's theory. These are transitions through virtual intermediate nuclear states which could compete with a forbidden direct transition leading, through destructive interference, to a lower intensity of the IB. Decay through the 430 keV, 2^+ state in ^{204}Hg , e.g., could constitute a large contribution to detour transitions. The γ rays in such transitions have a continuous spectrum since energy is not conserved in the intermediate state. In cases where the intermediate state is close in energy to the parent state, the detour transitions are expected to enhance the direct transitions for γ ray energies approaching the end-point energy of the spectrum, and thus can be observed as a high energy distortion of the IB spectrum.²² No such distortion has been observed in the present spectrum. Transitions through intermediate 1^- states in ^{204}Hg located at a higher energy could also contribute, since these would constitute a cascade of an allowed EC transition and an $E1$ transition. The magnitude of these contributions is expected to be small, however. Thus it is doubtful that detour transitions could explain the observed discrepancies between the theory and experiment in the present measurement.

This work was supported in part by the Faculty Award Program of the City University of New York.

¹P. Morrison and L. Schiff, Phys. Rev. **58**, 24 (1940).

²R. J. Glauber and P. C. Martin, Phys. Rev. **104**, 18 (1956).

³P. C. Martin and R. J. Glauber, Phys. Rev. **109**, 1307 (1958).

⁴W. Bambynek, H. Behrens, M. H. Chen, B. Craseman, M. L. Fitzpatrick, K. W. D. Ledingham, H. Genz, M. Mutterer, and R. L. Intemann, Rev. Mod. Phys. **49**, 77 (1977).

⁵B. A. Zon and L. P. Rapoport, Yad. Fiz. **7**, 528 (1968) [Sov. J. Nucl. Phys. **7**, 330 (1968)].

⁶B. A. Zon, Yad. Fiz. **13**, 963 (1971) [Sov. J. Nucl. Phys. **13**, 554 (1971)].

⁷B. Myslek, Z. Sujkowski, and J. Zylicz, Nucl. Phys. **A215**, 79 (1973).

⁸H. Lancman and A. Bond, Phys. Rev. C **1**, 2600 (1973), 15, 2257 (1977).

⁹H. Lancman and A. Zide (unpublished).

¹⁰R. E. Cutkosky, Phys. Rev. C **5**, 1222 (1954).

¹¹A. Bond and H. Lancman, Phys. Rev. C **6**, 2232 (1972).

¹²S. I. Salam, *Handbook of Chemistry and Physics* (CRC

Press, Cleveland, Ohio), 54th edition, p. E194.

¹³H. Lancman and J. M. Lebowitz, Phys. Rev. **188**, 1683 (1969).

¹⁴R. G. Jung and M. L. Pool, Bull. Am. Phys. Soc. **1**, 172 (1956).

¹⁵M. H. Biavati, S. J. Nassiff, and C. S. Wu, Phys. Rev. **125**, 1364 (1962).

¹⁶A. H. Wapstra and N. G. Gove, Nucl. Data **A9**, 265 (1971).

¹⁷B. A. Zon, Izv. Akad. Nauk SSSR Ser. Fiz. **37**, 1978 (1973) [Bull. Acad. Sci. USSR Phys. Ser. **37**, 153 (1973)].

¹⁸We wish to thank Professor R. Intemann at Temple Univ. for carrying out these calculations.

¹⁹C. Longmire, Phys. Rev. **75**, 15 (1949).

²⁰J. Horowitz, J. Phys. Rad. **13**, 429 (1952).

²¹G. W. Ford and C. F. Martin, Nucl. Phys. **A134**, 457 (1969).

²²M. E. Rose, R. Perrin, and L. L. Foldy, Phys. Rev. **128**, 1776 (1962).